Research Article • DOI: 10.2478/s13380-011-0001-x • Translational Neuroscience • 2(1) • 2011 • 23-32

Translational Neuroscience

VERSITA

GERSTMANN-STRAÜSSLER-SCHEINKER *PRNP P102L-129V* MUTATION

Isidro Ferrer[1,*],
Margarita Carmona[1],
Rosa Blanco[1],
Maria Jesus Rey Recio[2],
RM San Segundo[3]

[1]*Institut de Neuropatologia, Servei Anatomia Patològica, IDIBELL, Hospital Universitari de Bellvitge, Universitat de Barcelona, CIBERNED, Hospitalet de LLobregat, www.inpbellvitge.org;*

[2]*Banc de Teixits Neurologics, Hospital Clinic-Universitat de Barcelona, Barcelona;*

[3]*Centre Sociosanitari LLevant, Tarragona; Spain*

Abstract

Neuropathological and biochemical studies in a case of Gerstmann-Straüssler-Scheinker disease bearing the *PRNP P102L-129V* mutation showed numerous multicentric PrP^{res} in the cerebral cortex, striatum, thalamus and cerebellum, PrP^{res} globular deposits in the anterior and posterior horns of the spinal cord, and multiple granular PrP^{res} deposits in the grey and white matter of the encephalon and spinal cord. Western blots with antiPrP^{res} antibodies revealed several weak bands ranging from 36 to 66 kDa, weak bands of 29 and 24 kDa, a strong band of about 20 kDa, a low band of molecular weight around 15 kDa and a weaker band of about 7 kDa. Spongiform degeneration was absent. Hyper-phosphorylated 3R and 4R tau occurred in dystrophic neurites surrounding PrP^{res} plaques, neuropil threads and, to a lesser degree, in the form of neurofibrillary tangles. Gel electrophoresis of sarkosyl-insoluble fractions and western blotting with anti-phospho-tau antibodies showed a pattern similar to that seen in Alzheimer disease cases run in parallel. Dystrophic neurites in the vicinity of PrP^{res} plaques were enriched in voltage dependent anion channel thus suggesting abnormal accumulation of mitochondria. These changes were associated with increased oxidative damage in neurons and astrocytes, Finally, increased expression of active stress kinases, that have the capacity to phosphorylate tau *in vitro*, p38 (p-38-P) and SAPK/JNK (SAPK/JNK-P) was found in cell processes surrounding PrP plaques. Together, these observations provide evidences of mitochondrial abnormalities, and increased oxidative stress damage and oxidative stress responses in GSS bearing the *PRNP P102L-129V* mutation.

Keywords

Tau hyper-phosphorylation • Oxidative stress • SOD1 • SOD2 • Stress kinases p38 and SAPK/JNK • PrP • Creutzfeldt-Jakob • Gerstmann-Sträussler-Scheinker • Mitochondria

Received 31 December 2010
accepted 09 February 2011

1. Introduction

Prion diseases constitute a group of invariably fatal neurodegenerative disorders which are associated with the accumulation of proteinase K-resistant abnormal prion protein (PrP^{res}, PrP^{sc}) in the brain, leading to neuron loss and reactive astrocytic responses [1]. Prion diseases in animals include scrapie in goat and sheep, bovine spongiform encephalopathy in cattle, feline spongiform encephalopathy, chronic wasting disease in deer and spongiform encephalopathy in mink, as well as new atypical PrP animal disease forms [2,3]. In the human being, the most common prion disease is sporadic Creutzfeldt-Jakob disease (sCJD) [4,5]; a small percentage of human prion diseases are acquired by infection, including iatrogenic CJD and variant CJD (iCJD, vCJD, respectively) [1,6,7]. About 5-15% of human prion diseases are inherited and linked with disease-specific mutations in the prion protein gene (*PRNP*). These inherited forms include familial Creutzfeldt-Jakob disease (fCJD), Gerstmann-Straüssler-Scheinker disease (GSS) and fatal familial insomnia (FFI) [1]. The consequences of pathogenic mutations to the human prion protein and their effects on pathogenesis are still poorly understood [8, 9].

GSS disease is characterized by the presence of multicentric amyloid plaques derived from abnormal PrP products mainly distributed in the cerebral cortex, basal ganglia and cerebellum [10-13]. GSS is also distinguished in western blots by the presence of N- and C-terminal truncated PrP^{Sc} fragments ranging between 6 and 10 kDa and variable numbers of bands of higher molecular weight [13]. Most GSS cases are linked to *P102L* mutation in *PRNP*, but several additional mutations in *PRNP* are causative of GSS disease [1,13,14].

Importantly, although multicentric amyloid plaques derived from abnormal PrP products are constant features in GSS disease, patients suffering from certain *PRNP* mutations show, in addition, dramatic hyper-phosphorylated tau pathology [1,13]. Tauopathy mainly occurs in cases bearing the *F198S-129V* and *Q217R-129V* mutations [1,14-17]. Recently, we reported hyper-phosphorylated tau pathology in GSS linked with the *Y218N* mutation in *PRNP* [18].

Hyper-phosphorylated tau pathology in GSS is commonly manifested by neurofibrillary tangles throughout the cerebral cortex, neuropil threads and dystrophic neurites surrounding PrP^{res} plaques. Yet little is known about the band pattern of tau hyperphosphorylation in GSS and possible tau kinases involved in tau hyper-phosphorylation.

In addition to phospho-tau deposition around PrP plaques, dystrophic neurites, at least in the *Y218N PRNP* mutation, have strong immunoreactivity to membrane protein markers, such as voltage dependent anion channel (VDAC), thus indicating abnormal accumulation of altered mitochondria in the vicinity of PrP plaques [18].

* *E-mail: 8082ifa@gmail.com*

Whether this is a common feature in GSS with PrP plaques is not known.

Oxidative stress, altered oxidative stress responses and subsequent oxidative damage to brain DNA, RNA, lipids and proteins are constants in neurodegenerative diseases with abnormal protein aggregates. Oxidative RNA damage has been reported in sCJD [19] and increased lipid peroxidation occurs in experimental murine PrP^{res} disease, reaching its highest values at mid-incubation periods [20]. Increased concentrations of lipid peroxidation markers, and increased mRNA level of heme oxygenase-1, an oxidative stress response enzyme, have been demonstrated at relatively early stages of the disease in a murine model of scrapie [21]. Finally, increased glycoxidation (as revealed with N-carboxy-methyl lysine: CML, N-carboxy-ethyl-lysine: CEL), lipoxidation (as revealed with 4-hydroxynonenal: 4-HNE, and malondialdehyde lysine (MDAL); nitration (nitric oxide synthases nNOS, iNOS and eNOS; and nitrotyrosine: N-Tyr); and responses to oxidative stress (superoxide dismutase 1 and 2: SOD1 and SOD2) have been reported in the cerebral cortex in sCJD [22]. This is accompanied by alterations in brain lipid composition and increased amounts of glutamic and aminoadipic semialdehydes and products of metal-catalyzed oxidation [23]. In spite of this information concerning CJD and animal prion diseases, very limited data are available for GSS [19] and no information exists about possible protein targets of oxidative damage in GSS. This is important information as oxidation of most proteins results in impaired function [24], thereby aggravating disease phenotype.

The present study is based on a single GSS case bearing the *PRNP P102L-129V* mutation in which combined methods were used to characterize, not only PrP pathology, tau-hyperphosphorylation, but also mitochondrial damage, oxidative stress damage and oxidative stress responses.

2. Material and methods

2.1 Clinical findings

The patient was a 48-year-old woman institutionalized for last ten years with progressive neurological disability categorized as hereditary spastic paraparesia of Strümpell-Lorrain disease-type, cognitive impairment and, eventually, dementia with total external dependence, together with social uprooting, and lack of known relatives and friends. Seizures were not recorded at any time during her period of institutionalization. Genetic study evidenced *PRNP P102L-129V* mutation.

2.2 Neuropathological study

One hemisphere was immediately cut in coronal sections, 1 cm thick, frozen on dry ice and stored at -80º C until use. The other hemisphere was fixed by immersion in 4% buffered formalin for 3 weeks. Selected samples were treated with formic acid, and then post-fixed in formalin and embedded in paraffin. De-waxed sections were stained with haematoxylin and eosin and Klüver-Barrera, or processed for immunohistochemistry, following the En Vision+ system method. After incubation with methanol and normal serum, the sections were incubated with one of the primary antibodies overnight at 4ºC. Antibodies to glial fibrillary acidic protein (GFAP, Dako; Barcelona, Spain), b-amyloid (Boehringer-Mannheim; Barcelona, Spain) and ubiquitin (Dako) were used at dilutions of 1:250, 1:50, and 1:200, respectively. CD68 (Dako), used as a marker of microglia, was diluted at 1:100. AT8 antibody (Innogenetics; Barcelona, Spain) was used at a dilution of 1:50. Phospho-specific tau rabbit polyclonal antibodies Thr181, Ser202, Ser214, Ser262, Ser396 and Ser422 (all of them from Calbiochem, Barcelona, Spain) were diluted 1:100. Antibodies to 3R and 4R tau (Upstate, Millipore; Barcelona, Spain) were used at dilutions 1:800 and 1:50, respectively. Rabbit polyclonal anti-α-synuclein antibody (Chemicon; Barcelona, Spain) was used at a dilution of 1:3,000. TDP-43 was examined by using two different antibodies: a mouse monoclonal antibody (Abnova, Tebu-Bio; Barcelona, Spain) raised against a full-length recombinant human TARDBP, used at a dilution of 1:1,000, and a rabbit polyclonal antibody (Abcam; Cambridge, UK) raised against a synthetic peptide corresponding to C terminal (aa 350-414) of human TARDBP, used at a dilution of 1: 2,000. Monoclonal anti-αB-crystallin (Novocastra) was utilized at 1:50. Rabbit polyclonal anti-voltage dependent anion channel (VDAC; Abcam; Cambridge, UK) was diluted 1:100). The purified phospho-p38 MAP kinase (Thr180/Tyr182) (p38-P) rabbit polyclonal antibody (Cell Signaling; Danvers, MA, USA) detects p38 MAP kinase only when activated by dual phosphorylation at Thr180 and Tyr182. The purified rabbit polyclonal phospho-SAPK/JNK (Thr183/Tyr185) antibody (SAPK/JNK-P) (Cell Signaling) is produced against a synthetic phospho-Thr183/Tyr185 peptide corresponding to the residues of human SAPK/JNK. The antibody detects SAPK/JNK only when activated by phosphorylation at Thr183/Tyr185. Antibodies were used at a dilution of 1:200 and 1:150, respectively. Rabbit anti-glycogen synthase kinase-3β (GSK-3 βSer9; Oncogene; Cambridge, MA, USA) antibody was used diluted 1:100. Anti-prion protein antibody (antibody 3F4) (Dako, dilution 1:50) was incubated both treated and untreated with proteinase K. Rabbit polyclonal anti-HNE antibody (Calbiochem) was used at a dilution of 1:50. The goat antibody against the receptor of advanced glycation end products (RAGE; Serotec; Bloomington, MN, USA) at 1:500. Finally, the antibody against mutant ubiquitin (UBB+1) [25, 26], a generous gift of Dr. Fred W. van Leeuwen (Maastricht), was used at a dilution of 1:200.

The monoclonal anti-SOD1 antibody was used at dilution of 1:50 (Novocastra, Servicios Hospitalarios; Barcelona, Spain), and rabbit anti-SOD2 was diluted 1:100 (Stressgen, Bionova; Madrid, Spain). Following incubation with the primary antibody, the sections were incubated with EnVision + system peroxidase (Dako) for 15 min at room temperature. The peroxidase reaction was visualized with diaminobenzidine and H_2O_2. Control of the immunostaining included omission of the primary antibody; no signal was obtained following incubation with only the secondary antibody. Sections were slightly counterstained with haematoxylin.

2.3 Double-labeling immunofluorescence and confocal microscopy

De-waxed 5-micron-thick sections were stained with a saturated solution of Sudan black B (Merck; Barcelona, Spain) for 10 min to block the

autofluorescence of lipofuscin granules present in nerve cell bodies, rinsed in 70% ethanol, and washed in distilled water. The sections were incubated at 4ºC overnight with a combination of the primary antibodies to VDAC (Abcam) used at a dilution of 1:100, phospho-tau AT8 (Innogenetics) at 1:50; phospho-specific anti-tauThr181 (Calbiochem) at 1:150, and PrP (3F4) at 1:50.

After washing in PBS, the sections were incubated in the dark for 45 min at room temperature with a cocktail of secondary antibodies diluted in the same vehicle solution as the primary antibodies. Secondary antibodies were Alexa488 anti-rabbit or anti-mouse and Alexa555 anti-rabbit or anti-mouse (both from Molecular Probes; Leiden, Netherlands) used at a dilution of 1:400. Nuclei were stained with DRAQ 5 (Molecular Probes) diluted 1:2,000. Some sections were incubated only with the secondary antibodies. These sections were considered as negative controls. After washing in PBS, the sections were mounted in Immuno-Fluore Mounting medium (Sigma; Madrid, Spain), sealed, and dried overnight. Sections were examined with a Leica TCS-SL confocal microscope.

2.4 PrP immunoblotting

Frozen samples of the frontal cortex of GSS, two types I and II CJD cases and one control were processed in parallel for gel electrophoresis and western blotting with the PrP antibody 3F4 as detailed elsewhere [27, 28].

2.5 tau phosphorylation in sarkosyl-insoluble fractions

Frozen samples (of about 2 gr) from the frontal cortex of GSS and two typical Alzheimer's disease (AD) cases stage VC of Braak were gently homogenized in a glass tissue grinder in 10 vol (w/v) of cold suspension buffer (10mM TRIS-HCl, pH 7.4, 0,8M NaCl, 1mM EGTA, 10% sucrose, 20mM NaF, 25mM β-glycerophosphate, 10mM sodium pyrophosphate and protease inhibitor cocktail (Roche; Madrid, Spain). The homogenates were first centrifuged at 20,000 g and then the supernatant (S1) was retained. The pellet was re-homogenized in 5 vol of homogenization buffer and re-centrifuged. The two supernatants (S1+S2) were then mixed and incubated with 0.1% N-lauroylsarcosinate (sarkosyl) for 1h at room temperature while being shaken. Samples were then centrifuged at 100,000 g in a Ti70 Beckman rotor. Sarkosyl-insoluble pellets (P3) were re-suspended (0.2 ml/gr starting material) in 50 mM TRIS-HCl (pH 7.4). Western blot analyses were carried out with anti-phospho-tau Ser214 antibodies (Calbiochem) diluted 1:100.

2.6 Gel electrophoresis and western blotting

Samples containing 30 µgr of protein from the frontal cortex of GSS and three age- and sex-matched normal controls were loaded onto 10% acrylamide gels. Proteins were separated in sodium dodecyl sulphate (SDS)-polyacrylamide gel electrophoresis (PAGE) and electrophoretically transferred to nitrocellulose membranes (200 mA/membrane, 90 min). Subsequently, the membranes were washed with TBS (100mM Tris-buffered saline, 140mM NaCl, pH 7.4) and then incubated with a reducer solution of 10mM $NaBH_4$ in TBS for 30 min. After washing in TBS, the membranes were blocked with a solution of 5% skimmed milk in 100mM Tris-buffered saline, 140mM NaCl and 0.1% Tween 20, pH 7.4 (TBST buffer) for 1 h at room temperature. Then the membranes were incubated at 4º C overnight with one of the following antibodies: rabbit anti-cytochrome C oxidase (COX) subunit 4 (Molecular Probes, USA) diluted 1:2,000, mouse anti-ATP-synthase α chain antibody (Biosciences; Barcelona, Spain) used at a dilution of 1:1,000, rabbit polyclonal anti-4-hydroxynonenal (HNE) (Calbiochem, Bionova; Madrid, Spain) used at a dilution of 1:1,000, goat polyclonal malondialdehyde lysine (MDAL) (Academy Bio-Medical Company, Inc.; Houston, Texas) diluted 1:100, and anti-GFAP (rabbit polyclonal anti-GFAP, diluted 1: 500 or mouse monoclonal anti-GFAP antibody both from Dako used at a dilution of 1:10,000) in TBST containing 3% bovine serum albumin (BSA) (Sigma; Barcelona, Spain). In addition, mouse anti-Oxphos human (MitoProfile® Kit MS601, Mitosciences; Eugene, Oregon, USA) is composed of different antibodies, one against each of the 5 OXPHOS complexes. The mAbs are against complex I subunit NDUFB8, complex II subunit 30kDa, complex III subunit Core 2, complex IV subunit II, and ATP synthase subunit α. This was followed by incubation with horseradish peroxidase-conjugated secondary antibody (Dako) used at a dilution of 1:1,000, washing in TBST and development with the chemiluminescence ECL Hyperfilm (Amersham Biosciences). Membranes were scanned and saved in TIFF format using an HPLaserJet 3052.

2.7 2D gel electrophoresis and western blotting

Samples (0.25g) of the frontal cortex (area 8) of control and disease case were processed in parallel. 200mg of protein was mixed with 2D lysis buffer composed of 40mM Tris pH 7.5 containing 7M urea, 2M thiourea plus 0.2% Byolites (v/v), 4% CHAPS (Bio-Rad, Barcelona, Spain), 2mM TBP and 0.1% bromophenol blue in a final volume of 150µl.

In the first-dimension, sample solution was applied on immobilized 7cm IPG strips: pH 3-10 non-linear gradient, and pH 4-7 and pH 6-11, both linear gradient (Amersham Biosciences), at the basic and acidic ends of the strip. After re-hydration of the strips for 24 h, proteins were focused at 500V for 1 h, 1,000V for 8 h, 10,000V for 4 h and 50V for 5 h.

Strips were incubated in equilibration buffer (EB) composed of 50mM Tris-HCl pH 6.8, 6M urea, 1% SDS, 30% glycerol and 2% dithiothreitol (Sigma, Madrid, Spain). A second equilibration step was performed incubating strips for 10 min in EB containing 2.5% iodoacetamide (Biorad). All strips were placed onto 10% polyacrylamide gels and the second dimension gels were run at 0.02 A/gel. For gel staining, a MS-modified silver staining method (Amersham Biosciences) was used as described by the manufacturer. Control and the diseased cases were run in parallel. In every case, one gel was silver-stained while the other gel was transferred to a nitrocellulose membrane (200mA/membrane for 90 min). The anti-HNE antibody (Calbiochem) was used at a dilution of 1:1,000 in TBST containing 3% BSA.

2.8 In-gel digestion

Proteins were in-gel digested with trypsin (Sequencing grade modified, Promega, Barcelona, Spain) in the automatic Investigator ProGest robot of Genomic Solutions. Briefly,

excised gels spots were washed sequentially with ammonium bicarbonate buffer and acetonitrile. Proteins were reduced with 10mM dithiothreitol solution for 30 min and alkylated with 100mM solution of iodine acetamide for 15 min. After sequential washings with buffer and acetonitrile, proteins were digested overnight at 37° C with trypsin 0.27nM. Tryptic peptides were extracted from the gel matrix with 10% formic acid and acetonitrile. The extracts were pooled and dried in a vacuum centrifuge.

2.9 Acquisition of mass spectrometry and MS/MS spectra

Proteins manually excised from the 2D gels were digested and analyzed by CapLC-nano-ESI-MS-MS mass spectrometry. The tryptic digested peptide samples were analyzed using on-line liquid chromatography (CapLC, Micromass-Waters, Manchester, UK) coupled with tandem mass spectrometry (Q-TOF Global, Micromass-Waters). Samples were re-suspended in 12µl of 10% formic acid solution and 4µl was injected for chromatographic separation into a reverse-phase capillary C18 column (75µm internal diameter and 15cm in length, PepMap column, LC Packings, Amsterdam, The Netherlands). The eluted peptides were ionized via coated nano-ES needles (PicoTip™, New Objective, Woburn, MA, USA). A capillary voltage of 1,800–2,200V was applied together with a cone voltage of 80V. The collision in the collision-induced dissociation was 25–35 eV and argon was employed as the collision gas. Data were generated in PKL file format and submitted for database searching in MASCOT server (Matrix Science, Boston, MA, USA). NCBI database was used with the following parameters: trypsin enzyme, 1 missed cleavage, carbamidomethyl (C) as fixed modification and oxidized (M) as variable modification, and mass tolerance of 150–250 ppm

A probability-based MOWSE score was used to determine the level of confidence in the identification of specific isoforms from the mass spectra. This probability equals $10^{(\bullet \text{ MOWSE score}/10)}$. MOWSE scores greater than 50 were considered to indicate a high confidence of identification. All the experiments were done in triplicate

3. Results

3.1 Neuropathological findings

Gross examination of the brain revealed moderate, generalized cerebral atrophy and enlargement of the cerebral ventricles. The spinal cord was grossly unremarkable but Klüver-Barrera staining disclosed demyelination of the pyramidal lateral tracts and myelin pallor of the direct pyramidal tract.

Microscopical examination revealed moderate-to-severe neuronal loss in the cerebral cortex, basal ganglia, nuclei of the anterior prosencephalon and amygdala. Discrete neuronal loss was observed in the granular layer of the cerebellum, substantia nigra and reticular formation of the brain stem. Purkinje cells were preserved. Motor neurons of the motor nuclei of the brain stem and anterior horn of the spinal cord were apparently not affected. Numerous multicentric plaques were seen with haematoxylin and eosin and PAS stains throughout the encephalon (Figure 1a-c). Plaques were best seen with PrP antibodies (3F4 clone) and were resistant to proteinase K (PK) treatment. Abundant plaques were found in the cerebral cortex, striatum, thalamus and cerebellum (mainly in the molecular layer) (Figure 1d-h). PK resistant PrP globular deposits were also present in the anterior and posterior horns of the spinal cord (Figure 1i). In addition, multiple granular PrP deposits were widespread in the grey and white matter of the encephalon and spinal cord (Figure 2a). Spongiform degeneration was absent.

Microscopical study also disclosed increased numbers of astrocytes in the neuropil, many of them in the vicinity of PrP plaques (Figure 2b). Increased numbers of active microglial cells were distributed at random (Figure 2c). Many neurons and reactive astrocytes disclosed increased αB-crystallin immunoreactivity (Figure 2d). A most dramatic picture was seen with phospho-specific anti-tau antibodies. Numerous abnormal neurites surrounding PrP plaques were stained with anti-phospho-tau antibodies, either using clone AT8 (Figure 2e,f) or specific rabbit polyclonal anti-tau Thr181, Ser202, Ser262, Ser396 and Ser422 antibodies (data not shown). Dystrophic

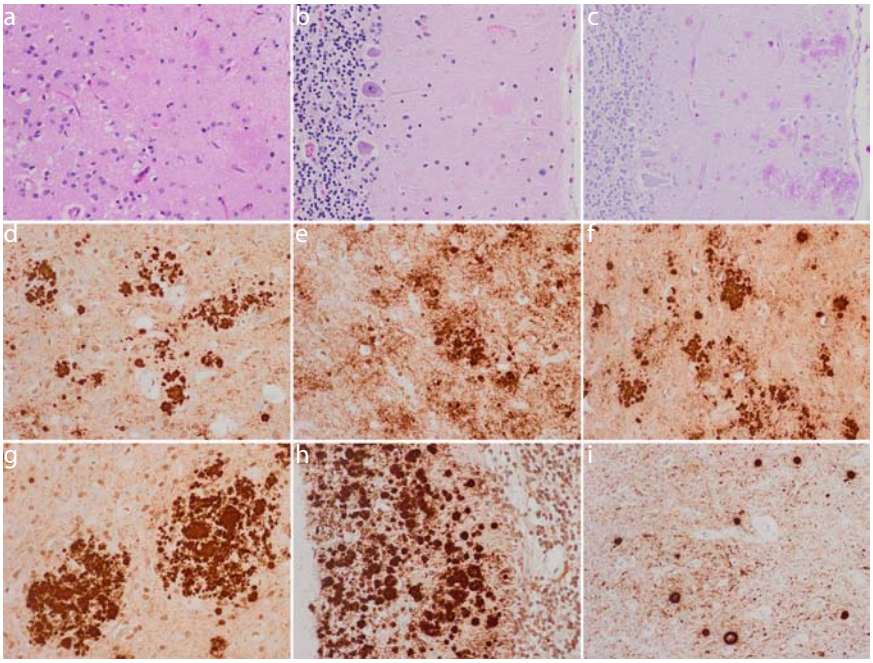

Figure 1. Multicentric plaques are seen with haematoxylin and eosin in the cerebral cortex (a) and cerebellum (b), which are stained with the PAS method (c). Plaques, stained with anti-PrP antibodies following pre-treatment with proteinase K (PK), are found in the frontal cortex (d), temporal cortex (e), striatum (f), thalamus (g) and cerebellum (h). PK-resistant PrP deposits are also observed in the anterior horn of the spinal cord (i). D-I: Paraffin sections slightly counter-stained with haematoxylin.

neurites were stained with anti-3R tau and with anti-4R tau, indicating that 3R and 4R tau were components of dystrophic neurites surrounding plaques (Figure 2g,h). Dystrophic neurites were also stained with anti-ubiquitin antibodies (Figure 2i), suggesting impairment of the ubiquin-protesome system (UPS) of protein degradation in dystrophic neurites of PrP plaques. This was further supported by the presence of mutant ubiquitin (UBB+) in dystrophic neurites (data not shown). In addition to altered neurites, several neurons also disclosed hyper-phosphorylated tau pathology (data not shown).

Double-labelling immunofluorescence and confocal microscopy further supported the close association (without cellular co-localization) of PrP multicentric plaques and hyper-phosphorylated tau (data not shown).

Confocal microscopy analysis also disclosed the presence of abnormal VDAC in association with multicentric plaques (Figure 3), thus suggesting abnormal accumulation of altered mitochondria in cellular processes in the vicinity of PrP plaques. Similar profiles were observed in the cerebrum and cerebellum (data not shown).

b-amyloid plaques were absent. Abnormal α-synuclein and TDP-43 deposits were not seen in any region.

Immunohistochemistry to oxidative stress markers and oxidative stress responses showed increased HNE immunoreactivity in neurons (Figure 4b) and astrocytes (Figure 4e), increased peroxiredoxin in neurons and glial cells (Figure 4c), increased RAGE in glial cells (mainly microglia) (Figure 4d) and increased SOD2 in astrocytes (Figure 4f). All these events were clearly not related with PrP multicentric plaques (Figure 4a). In contrast, increased SOD1 immunoreactivity occurred in association with PrP plaques (compare the distribution of PrP and SOD1 in Figures 4a and 4g, respectively). Moreover, increased active p38 (p-38-P) and SAPK/JNK (SAPK/JNK-P) expression was found in cell processes surrounding PrP plaques (Figure 4h,i). Similar results were obtained with anti-GSK-3β antibodies (data not shown). Together, these observations suggest widespread increase of oxidative stress damage and oxidative stress responses in GSS, and activation of SOD1 and stress kinases p38 and SAPK/JNK in association with PrP multicentric plaques.

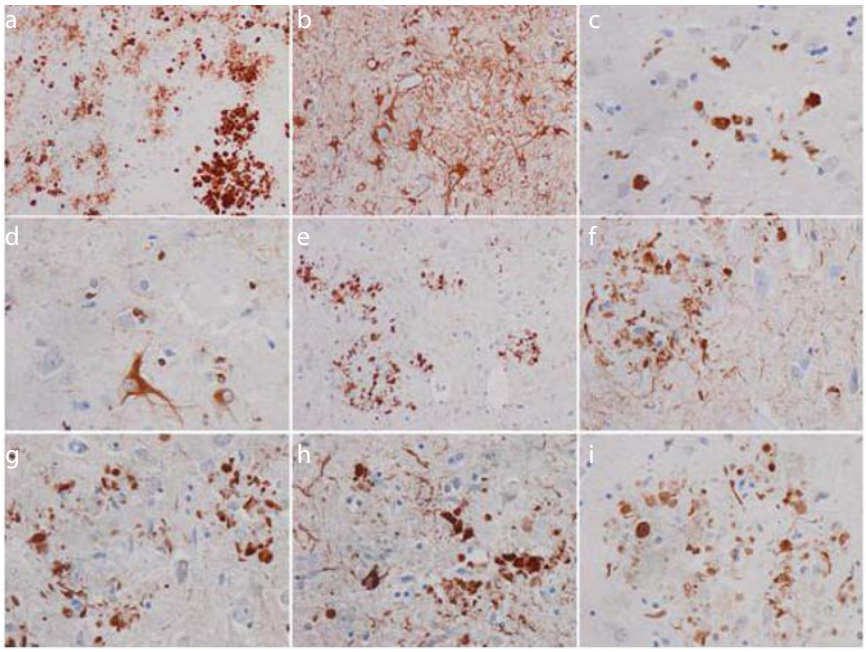

Figure 2. In addition to multicentric plaques, granular PrP deposits are widespread in the grey matter (a). Increased numbers of astrocytes are seen in the vicinity of PrP plaques (b), active microglial cells distributed at random (c) and increased αB-crystallin immunoreactivity in isolated neurons (d). Abnormal neurites, surrounding PrP plaques, are stained with anti-phospho-tau antibodies (clone AT8) (e, f). Dystrophic neurites are also decorated with anti-3R tau (g) and anti anti-4R tau antibodies (h). Dystrophic neurites are stained with anti-ubiquitin antibodies (i). Paraffin sections slightly counter-stained with haematoxylin.

3.2 PrP type

The PrP pattern of GSS case on western blots was different from the typical CJD band patterns type I and type II run in parallel. *PRNP P102L-129V* case disclosed weak bands (when compared with type I and type II) of PK-resistant PrP of 29 and 24 kDa, a strong band of about 20 kDa, a low band of molecular weight around 15 kDa and a weaker band of about 7 kDa. Several weak bands ranging from 36 to 66 kDa were also present (Figure 5a).

3.3 tau hyperphosphorylation

Gel electrophoresis of sarkosyl-insoluble fractions and western blotting with antiphospho-tau Ser 214 antibodies showed three upper bands of 68, 64 and 60 kDa together with several bands of lower molecular weight of about 40, 35 and 25 kD in stage VC AD cases (Figure 6). GSS sample processed in parallel showed the three upper bands, the one of about 60 kDa being composed of a doublet. Bands of lower molecular weight were barely identified with this exposure. Yet longer exposure resulting in saturation of the bands in AD cases permitted the visualization of bands of 35 and 25 kDa in the GSS case (Figure 5b).

3.4 Altered mitochondrial profile

Western blots showed no differences in the expression levels of ATP synthase α chain between controls and the GSS case. Expression levels of sub-units of complexes I NUDUFB8 (20 kDa), III subunit core 2 (47 kDa) and V (α chain, 50 kDa), as revealed by Oxphos labelling, were not affected in GSS. No labelling was obtained for complex IV subunit II and complex II subunit of 30 kDa. However, altered expression of COX subunit 4 was seen in GSS when compared with controls as a band of lower molecular weight, in addition to the 50 kDa band observed in controls, suggesting abnormal formation or assembly of COX subunit 4 (Figure 6).

3.5 Identification of proteins affected by oxidative damage

Western blots to HNE showed several weak bands in controls but strong bands between

37 and 50 kDA and 100 kDa in the GSS case. Western blots also disclosed increased intensity of MDAL in the GSS case when compared with age-matched controls although with a different pattern to that seen with HNE. Interestingly, the strong HNE bands between 37 and 50 kDa in GSS were similar to those obtained in western blots to GFAP, suggesting that GFAP might be one of the proteins modified by HNE adducts. To identify HNE-modified proteins in the GSS case, bi-dimensional gel electrophoresis, western blotting and mass spectrometry was performed in the GSS and control cases; GFAP was identified as an HNE-modified protein (coverage: 86.57, number of peptides matching: 59, score: 236).

4. Discussion

Clinical symptoms in the present case differ from those reported in GSS cases bearing the *P102L PRNP* mutation [6, 12, 13, 17, 29, 30]. Cases with *PRNP P102L-129M* suffer from progressive cerebellar syndrome, pyramidal signs, pseudo-bulbar palsy and cognitive impairment followed by dementia, whereas cases with *PRNP P2102L-129V* show spastic paraparesia and seizures, but not dementia. Spastic paraparesia was the main symptom in this case suggesting a diagnosis of Strümpell-Lorrain disease on the basis of similar pyramidal signs in the patient's family, followed by cognitive impairment and severe dementia. Thus, there appears to be a combined clinical phenotype in this particular case. This further supports marked clinical heterogeneity in GSS even in those carrying the same mutation [30-32].

Neuropathological examination revealed multicentric PrP plaques throughout the encephalon, including the cerebellum, and degeneration of the pyramidal tracts, with no spongiform degeneration. PrP^{res} typing in the present case is reminiscent of that seen in other GSS cases, including the presence of full-length, truncated and aggregated forms of PrP^{res} [1, 11, 33-35].

Hyper-phosphorylated tau accumulation in relation with PrP^{res} deposits accompanied by neurofibrillary tangles and neuropil threads is common in GSS cases bearing certain *PRNP* mutations such as the *F198S-129V, Q217R-129V, H187R-129V* and *Y218N* mutations in *PRNP* [1, 14-18, 36]. Rarely, tauopathy has also been described in GSS linked with the *P102L* mutation [37] as in the case with *P102L-129V* in the present study. Tauopathy may also occur in human and experimental variants of Creutzfeldt-Jakob disease [38, 39]. Certain PrP mutants have stronger binding activity with tau than wild PrP [40], but this aspect does not appear to be sufficient to explain neurofibrillary tangle pathology and neuropil threads in GSS cases. Severe neuritic pathology with hyper-phosphorylated tau accumulation, rather than neurofibrillary tangle pathology, was prominent in the present case. This was composed of 3R and 4R tau isoforms, and western blots of sarkosyl-insoluble fractions revealed a band pattern of tau hyper-phosphorylation characterized by three bands of 68, 64 and 60 kDa, and several bands of lower molecular of about 40, 35 and 25 kDa. This pattern is the same as in Alzheimer's disease (AD) [41, 42].

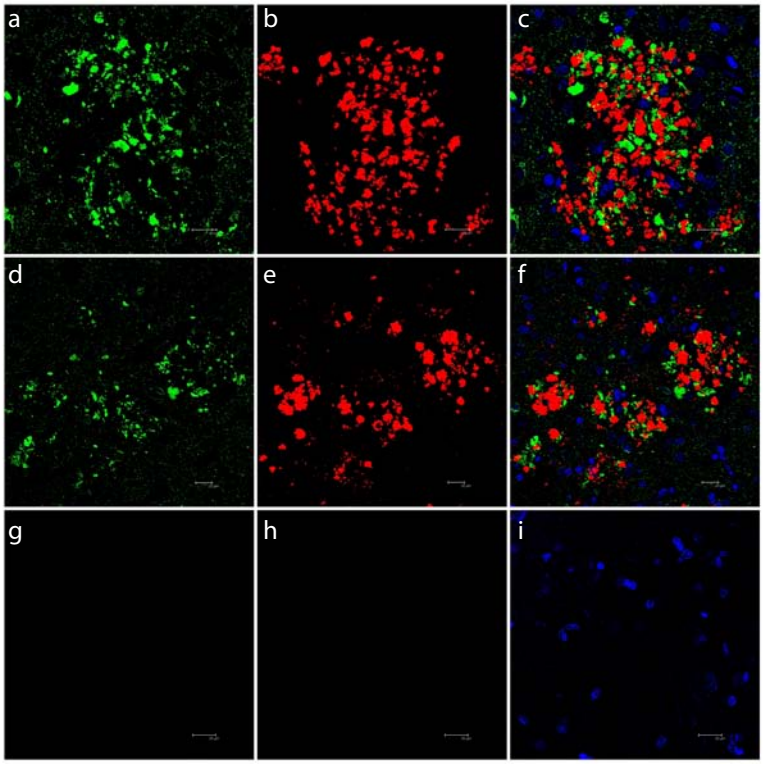

Figure 3. Double-labelling immunofluorescence and confocal microscopy show large granular VDAC-immunoreactive deposits (green) in association with PrP plaques (red) in several regions including cerebral cortex (a-c) and cerebellum (d-f). c, f and i: merge. g-i are sections incubated without the primary antibodies to rule out non-specific immunofluorescence. Note the very fine granular green immunostaining corresponding to normal mitochondria in the neuropil in comparison to the abnormal granular accumulation of VDAC in relation with PrP plaques.

The reasons for the occurrence of tau hyper-phosphorylation in AD and other tauopathies seem to depend on several factors including hyperactivity of tau-specific kinases and reduced function of certain phosphatases. Active stress kinases SAPK/JNK (SAPK/JNK-P) and p38 (p38-P) are commonly implicated in tau hyper-phosphorylation in AD and other tauopathies [43-45]. SAPK/JNK-P and p38-P are similarly expressed in hyper-phosphorylated tau dystrophic neurites in association with PrP plaques, suggesting a link between activation of stress kinases in tau phosphorylation in the GSS case as already observed in AD and related transgenic models [46].

Hyper-phosphorylated tau accumulation also depends on altered function of the UPS of protein degradation. In favour of altered

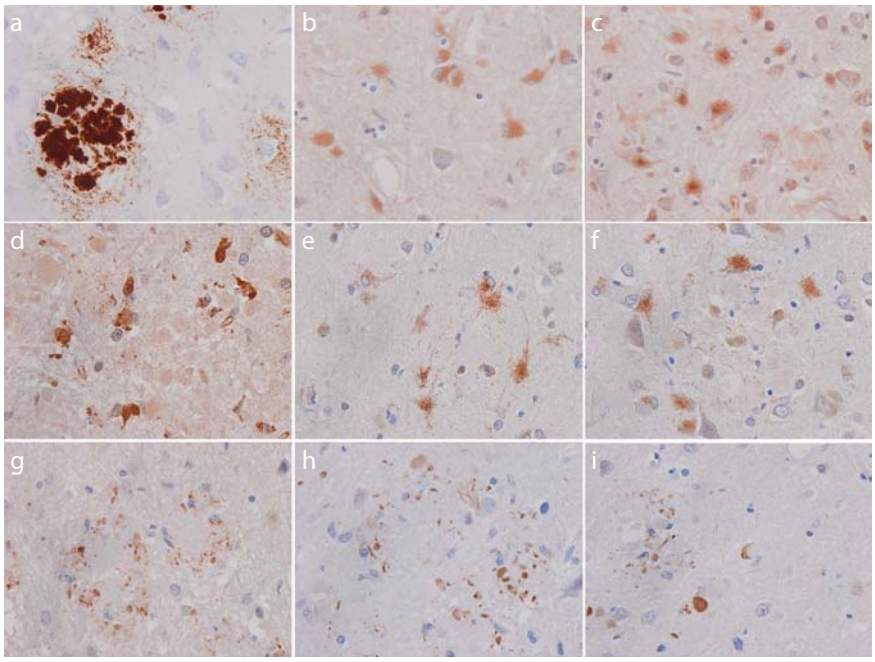

Figure 4. Immunohistochemistry to oxidative stress markers and oxidative stress responses show increased HNE immunoreactivity in neurons (b) and astrocytes (e), increased peroxiredoxin in neurons and glial cells (c), increased RAGE in microglia (d) and increased SOD2 in astrocytes (f). All these events are clearly not related with PrP multicentric plaques (a). In contrast, increased SOD1 immunoreactivity occurs in association with PrP plaques (g). Increased active p38 (p-38-P) and SAPK/JNK (SAPK/JNK-P) immunoreactivity is found in cell processes surrounding PrP plaques (h, i, respectively). Paraffin sections slightly counter-stained with haematoxylin.

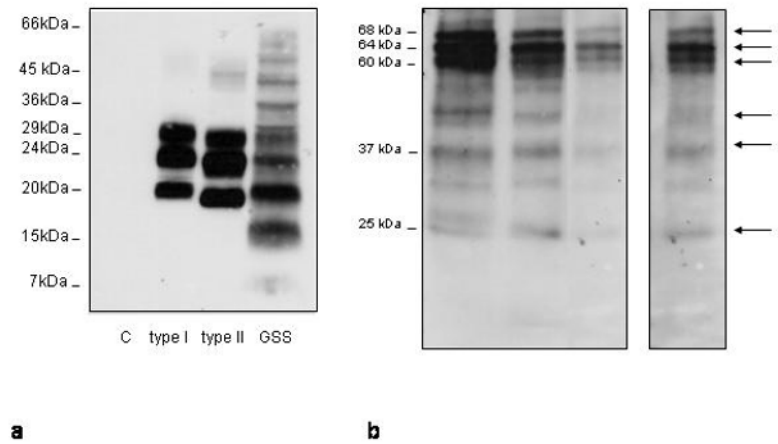

Figure 5. Gel electrophoresis and western blotting of proteinase K-resistant PrP shows bands of 29, 24, 20, 15 and about 7 kDa, and several weak bands ranging from 36 to 66 kDa in the GSS case following a pattern very different from classical CJD types I and II run in parallel. Control brain (C) is negative (a). Gel electrophoresis of sarkosyl-insoluble fractions and western blotting with anti-phosphorylated tau antibodies (Ser214) show three upper bands of 68, 64 and 60 kDa together with several bands of lower molecular weight of about 40, 35 and 25 kD in stage VC AD cases. The same type of band is found in the GSS case although the lower bands are only seen after a long exposure time (separate lane on the right) (b).

function of the UPS in the present case is the presence of ubiquitin in dystrophic neurites bearing hyper-phosphorylted tau. Furthermore, mutant ubiquitin (UBB+), resulting from misreading of the ubiquitin B gene, has the capacity to bind to altered proteins, but at high concentrations, and this inhibits the proteasome [25, 47, 48]. This aspect does not appear to be restricted to the present case, as aberrant UBB+ in relation with tau hyperphosphorylation has been observed in another GSS case with hyper-phosphorylated tau pathology bearing the PRNP Y218N mutation [18].

Mitochondrial abnormalities and residual mitochondria in autophagic vacuoles are seen in dystrophic neurites of senile plaques in AD [49-52]. In addition, abnormalities in the expression levels or in the functional activities of selected proteins of mitochondrial complexes of the respiratory chain appear to be early alterations in AD brains [53-55]. Altered mitochondria in cell processes in the vicinity of PrP plaques have also been previously observed in GSS [18] and they are further confirmed in the present case. Moreover, abnormal expression of cytochrome C oxidase sububnit IV, but not of other subunits of the oxidative phosphorylation multicomplex, indicates selective alteration of complex IV in GSS, similar to that seen in AD [53]. It is worth stressing that cytochrome C oxidase subunit IV is essential to the assembly and respiratory function of the enzyme complex [56].

Oxidative stress and oxidative stress damage to proteins, albeit with different characteristics and targets, are common in the majority of, if not all, degenerative diseases of the nervous system [57, 58]. Oxidative stress damage has also been reported in human and animal prion diseases [19, 21-23]. The present findings have shown, by western blotting, increased HNE and MDAL adducts in GSS when compared with age-matched controls. As demonstrated by immunohistochemistry, HNE adducts are present in neurons and astrocytes, whereas markers of oxidative stress responses appear to be cell-dependent: peroxiredoxin in neurons, RAGE (receptor of advanced glycation end products) in microglia, SOD2 in astrocytes and SOD1 in cellular processes (probably

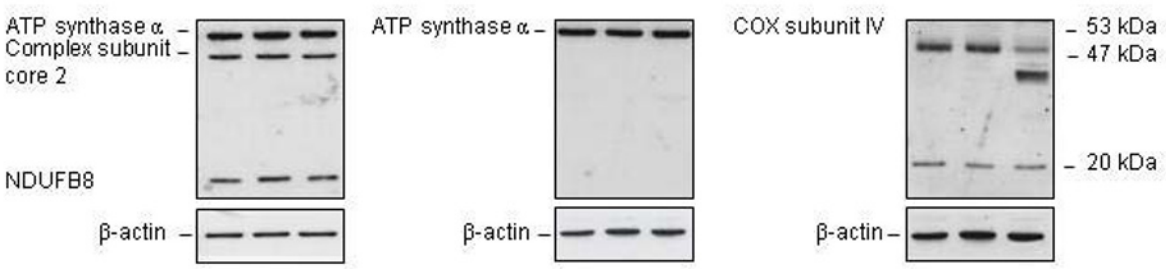

Figure 6. Western blots show no differences in the expression levels of ATP synthase α chain (complex V), NUDUFB8 subunit (complex I) and subunit core 2 (complex III) between controls and the GSS case. COX subunit 4 is represented by a weak band of about 20 kDa and an upper band of about 50 kDa in controls. Yet GSS shows a decreased upper band of 50 kDa at the expense of a band of lower molecular weight of about 45 kDa, suggesting abnormal expression of COX subunit 4.

aberrant neurites) in the vicinity of PrP plaques. Therefore, the present observations show, for the first time, a plethora of oxidative stress damage and oxidative stress responses in GSS, and reinforce the hypothesis that redox imbalance and oxidative stress contribute to PrP pathogenesis [59].

Oxidative stress may have an impact on different molecules. A prominent target is glial fibrillary acidic protein (GFAP). This protein is also oxidatively damaged in other degenerative diseases of the nervous system, including Alzheimer's disease, progressive supranuclear palsy, Pick's disease and frontotemporal lobar degeneration [60-64].

In summary, the present observations point to a sequence of events triggered by mutant PrP deposition in plaques which results in the mitochondrial damage of cellular processes in the vicinity of PrP deposits. This, in turn, may be causative of increased production of reactive oxygen species, increased oxidative stress responses and increased oxidative damage that targets various proteins including astrocytic proteins (i.e. GFAP); and of activation of stress kinases which may hyper-phosphorylate 3R and 4R tau. Hyper-phosphorylated tau (also phosphorylated by other kinases as GSK-3β) is bound to ubiquitin and mutant ubiquitin (UBB+) resulting in UPS blocking. Hyper-phosphorylated tau then accumulates in neurites around PrP plaques, neuropil threads and neurofibrillary tangles.

Acknowledgements

This study was carried out in part with the support of Neuroprion (EU 2004 Food CT-2004-506579) and FIS grant IP08-0582. We thank T Yohannan for editorial assistance.

References

[1] Ironside JW, Ghetti B, Head MW, Piccardo P, Will RG, Prion diseases. In: Love S, Louis DN, Ellison DW (eds) Greenfield's Neuropathology. London: Hodder Harnold, 2008, pp 1197-1274

[2] Aguzzi A, Prion diseases of humans and farm animals: epidemiology, genetics, and pathogenesis, J Neurochem 2006, 97, 1726-1739

[3] Yokoyama T, Mohri S, Prion diseases and emerging prion diseases, Curr Med Chem, 2008, 15, 912-916

[4] Budka H, Head MW, Ironside JW et al., Sporadic Creutzfeldt-Jakob disease. In: Dickson D (ed) Neurodegeneration: The molecular pathology of dementia and movement disorders, ISN Neuropath Press, Basel, 2003, pp 287-297

[5] Ironside JW, Head MW, Biology and neuropathology of prion diseases. In:Duyckaerts C, Litvan I (eds) Handbook of Clinical Neurology vol 39. Edinburgh, London, New York, Oxford, Philadelphia, St Louis, Sydney, Toronto, 2008, pp779-797

[6] Ironside JW, Head MW, Will RG, Variant Creutzfeldt-Jakob disease. In: Dickson D (ed) Neurodegeneration: The molecular pathology of dementia and movement disorders. Basel: ISN Neuropath Press, 2003, pp 310-306

[7] Ricketts MN, Pergami P, Iatrogenic prion disorders. In: Dickson D (ed) Neurodegeneration: The molecular pathology of dementia and movement disorders, ISN Neuropath Press, Basel, 2003, pp 307-309

[8] van der Kamp MW, Daggett V, The consequences of pathogenic mutations to the human prion protein, Protein Eng Des Sel, 2009, 22, 461-468

[9] Solomon IH, Schepker JA, Harris DA, Prion neurotoxicity: insights from prion protein mutants, Curr Issues Mol Biol, 2010, 2, 51-61

[10] Gerstmann J, Straussler E, Scheinker I, Über eine eigenartige hereditär-familiäre Erkrankung des Zentralnervensystems. Zugleich ein Beitrag zur Frage des vozeitigen lokalen Alterns, Zeitscher Neurol Psychiatr, 1936, 154, 736-762

[11] Ghetti B, Dlouhy SR, Giaconne G et al., Gerstmann-Sträussler-Scheinker disease and the Indiana kindred, Brain Pathol, 1995, 5, 61-75

[12] Young K, Clark HB, Piccardo P et al., Gerstmann-Sträussler-Scheinker disease with the PRNP P102L mutation and valine at codon 129, Brain Res Mol Brain Res, 1997, 44, 147-150

[13] Ghetti B, Bugiani O, Tagliavini F, Piccardo P, Gerstmann-Straüssler-Scheinker disease. In: Dickson DW (ed) Neurodegeneration: the molecular pathology of dementia and movement disorders. ISN Neuropath Press, Basel, 2003, pp 318-325

[14] Kong Q, Surewicz W, Petersen RB et al., Inherited prion diseases. In: Prusiner SB, ed. Prion biology and diseases. New York: Cold Spring Harbor Laboratory Press, 2004, pp 673-776

[15] Ghetti B, Tagliavini F, Masters CL et al., Gerstmann-Straüssler-Scheinker disease. II. Neurofibrillary tangles and plaques with PrP deposits coexist in an affected family, Neurology, 1999, 39, 1453-1461

[16] Guetti B, Tagliavini F, Giaconne G et al., Familial Gerstmann-Straüssler-Scheinker disease with neurofibrillary tangles, Mol Neurobiol, 1994, 8, 41-48

[17] Ghetti B, Piccardo P, Frangione B et al., Prion protein amyloidosis, Brain Pathol, 1996, 6, 127-145

[18] Alzualde A, Indakoetxea B, Ferrer I et al., A novel PRNP Y218N mutation in Gerstmann-Straüssler-Scheinker disease with neuroifibrillary degeneration, J Neuropathol Exp Neurol, 2010, 69, 789-800

[19] Petersen RB, Siedlak SL, Lee HG et al., Redox metals and oxidative abnormalities in human prion diseases, Acta Neuropathol, 2005, 110: 232-238

[20] Brazier MW, Lewis V, Ciccotosto GD et al., Correlative studies support lipid peroxidation is linked to PrP(res) propagation as early primary pathogenetic event in prion disease, Brain Res Bull, 2006, 68, 346-354

[21] Yun SW, Gerlach M, Riederer P, Klein MA, Oxidative stress in the brain at early preclinical stages of mouse scrapie, Exp Neurol, 2006, 201, 90-98

[22] Freixes M, Rodriguez A, Dalfo E, Ferrer I, Oxidation, glycoxidation, lipoxidation, nitration, and stress in the cerebral cortex in Creutzfeldt-Jakob disesae, Neurobiol Aging, 2006, 27, 1807-1815

[23] Pamplona R, Naudi A, Gavín R et al, Increased oxidation, glycoxidation, and lipoxidation of brain proteins in prion disease, Free Radic Biol Med, 2008, 45, 1159-1166

[24] Cabiscol E, Ros J, Oxidative damage to proteins: Structural modifications and consequences in cell function. In: Dalla-Donne I, Scaloni A, Butterfield A (eds). Redox proteomics. From protein modifications to cellular dysfunction and diseases. John Wiley and Sons, New Jersey, 2006, pp 399-472

[25] van Leeuwen FW, de Kleijn DP, van den Hurk HH et al., Frameshift mutants of beta amyloid precursor protein and ubiquitin-B in Alzheimer's and Down patients, Science, 1998, 279, 242-247

[26] Fischer DF, De Vos RA, Van Dijk R, et al., Disease-specific accumulation of mutant ubiquitin as a marker for proteasomal dysfunction in the brain, FASEB J, 2003, 17, 2014-2024

[27] Notari S, Capellari S, Langeveld J et al., A refined method for molecular typing reveals that co-occurrence of PrP(Sc) types in Creutzfeldt-Jakob disease is not the rule, Lab Invest, 2007, 87, 1103-1112

[28] Parchi P, Notari S, Weber P et al., Inter-laboratory assessment of PrPSc typing in Creutzfeldt-Jakob disease: a Western blot study within the NeuroPrion Consortium, Brain Pathol, 2009, 19, 384-391

[29] Bianca M, Bianca S, Vecchio I et al., Gerstmann-Sträussler-Scheinker disease with P102L-V129 mutation: A case with psychiatric manifestations at onset, Am Genet, 2003, 46, 467-469

[30] Webb TE, Poulter M, Beck J et al., Phenotypic heterogeneity and modifications of P102L inherited prion disease in an international series, Brain, 2008, 131, 2632-2646

[31] Wadsworth JD, Joiner S, Linehan JM et al., Phenotypic heterogeneity in inherited prion disease ((P102L) is associated with differential propagation of protease-resistant wild-type and mutant prion protein, Brain, 2006, 129, 1557-1569

[32] Giovagnoli AR, Di Fede G, Aresi A et al. Atypical frontotemporal dementia as a new clinical phenotype of Gerstmann-Srtaüssler-Scheinker disease with the PRNP P102L mutation. Description of a previously unreported Italian family, J Neurol Sci, 2008, 29, 405-410

[33] Piccardo P, Dlouhy SR, Lievens PM et al., Phenotypic variability of Gerstmann-Sträussler-Scheinker disease is associated with prion protein heterogeneity, J Neuropathol Exp Neurol, 1998, 57, 979-988

[34] Parchi P, Chen SG, Brown P et al., Different patterns of truncated prion protein fragments correlate with distinct phenotypes in P102L Gerstmann-Straussler-Scheinker disease, Proc Natl Acad Sci U S A, 1998, 95, 8322-8327

[35] Hill AF, Joiner S, Beck JA et al., Distinct glycoform ratios of protease resistant prion protein associated with PRNP point mutations, Brain, 2006, 129, 676-685

[36] Colucci M, Xie Z, Butefisch CM et al., A novel mutation in the prion protein gene associated with distinct pathology, Brain Pathol, 2000, 10, 672

[37] Ishizawa K, Komori T, Shimazu T et al., Hyperphosphorylated tau deposition parallels prion protein burden in a case of Gerstmann-Sträussler-Scheinker syndrome P102L mutation complicated with dementia, Acta Neuropathol, 2002, 104, 342-350

[38] Giaconne G, Mangieri M, Capobianco R et al., Tauopathy in human and experimental variant Creutzfeldt-Jakob disease, Neurobiol Aging, 2008, 29, 1864-1873

[39] Sikorska B, Liberski PP, Sobow T et al., Ultrastructural study of florid plaques in variant Creutzfeldt-Jakob disease: a comparison with amyloid plaques in kuru, sporadic Creutzfeldt-Jakob disease and Gerstmann-Straüssler-Scheinker disease, Neuropathol Appl Neurobiol, 2009, 35, 46-59

[40] Wang XF, Dong CF, Zhang J et al., Human tau protein forms complex with PrP and some GSS- and fCJD-related PrP mutants possess stronger binding activities with tau in vitro, Mol Cell Biochem, 2008, 310, 49-55

[41] Goedert M, Introduction to the tauopathies. In: Dickson D (ed) Neurodegeneration: The molecular pathology of dementia and movement disorders, ISN Neuropath Press, Basel, 2003, pp 82-85

[42] Santpere G, Puig B, Ferrer I, Low molecular weight species of tau in Alzheimer's disease are dependent on tau phosphorylation sites but not on delayed post-mortem delay in tissue processing, Neurosci Lett, 2006, 399, 106-110

[43] Atzori C, Ghetti B, Piva R et al., Activation of the JNK/p38 pathway occurs in diseases characterized by tau protein pathology and is related to tau phosphorylation but not to apoptosis. J Neuropathol Exp Neurol, 2001, 60, 1190-1197

[44] Ferrer I, Blanco R, Carmona M, Puig B, Phosphorylated mitogen-activated protein kinase (MAPK/ERK-P), protein kinase of 38 kDa (p38-P), stress-activated protein kinase (SAPK/JNK-P), and calcium/calmodulin-dependent kinase II (CaM kinase II) are differentially expressed in tau deposits in neurons and glial cells in tauopathies, J Neural Transm, 2001, 108, 1397-1415

[45] Ferrer I, Gomez-Isla T, Puig B et al., Current advances on different kinases involved in tau phosphorylation, and implications in Alzheimer's disease and tauopathies, Curr Alzheimer Res, 2005, 2, 3-18

[46] Ferrer I, Stress kinases involved in tau phosphorylation in Alzheimer's disease, tauopathies and APP transgenic mice, Neurotox Res, 2004, 6, 469-475

[47] de Pril R, Fisher DF, van Leewen FW, Conformational diseases: an umbrella for various neurological disorders with an impaired ubiquitin-proteasome system, Neurobiol Aging, 2006, 27, 515-523

[48] van Tijn P, de Vrij FM, Schuurman KG et al., Dose-dependent inhibition of proteasome activity by a mutant ubiquitin associated with neurodegeneartive disease, J Cell Sci, 2007, 120, 1615-1623

[49] Kidd M, Alzheimer's Disease -- an electron microscopical study, Brain, 1964, 87,307-320

[50] Luse SA, Smith KR (1964) The ultrastructure of senile plaques. Am J Pathol 44: 553-563

[51] Terry RD, Gonatas NK, Weiss M, Ultrastructural studies in Alzheimer's presenile dementia, Am J Pathol, 1964, 44, 269-297

[52] Hirai K, Aliev G, Nunomura A et al., Mitochondrial abnormalities in Alzheimer's disease, J Neurosci, 2001, 21, 3017-3023

[53] Pérez-Gracia E, Torrejón-Escribano B, Ferrer I, Dystrophic neurites of senile plaques in Alzheimer's disease are deficient in cytochrome c oxidase, Acta Neuropathol, 2008, 116, 261-268

[54] Ferrer I, Altered mitochondria, energy metabolism, voltage-dependent anion channel, and lipid rafts converge to exhaust neurons in Alzheimer's disease, J Bioenerg Biomembr, 2009, 41, 425-431

[55] Terni B, Boada J, Portero-Otin M, Pamplona R, Ferrer I, Mitochondrial ATP-synthase in the entorhinal cortex is a target of oxidative stress at stages I/II of Alzheimer's disease pathology, Brain Pathol, 2010, 20, 222-233

[56] Li Y, Park JS, Deng JH, Bai Y (2006) Cytochrome c oxidase subunit IV is essential for assembly and respiratory function of the enzyme complex. J Bioenerg Biomembr 38: 283-291

[57] Sultana R, Perluigi M, Butterfield DA, Oxidatively modified proteins in Alzheimer's disease (AD), mild cognitive impairment and animal models of AD: role of Abeta in pathogenesis, Acta Neuropathol, 2009, 118, 131-150

[58] Martínez A, Portero-Otin M, Pamplona R, Ferrer I, Protein targets of oxidative damage in human neurodegenerative diseases with abnormal protein aggregates, Brain Pathol, 2010, 20, 281-297

[59] Singh N, Singh A, Das D, Mohan ML, Redox control of prion and disease pathogenesis, Antioxid Redox Signal, 2010, 12, 1271-1294

[60] Korolainen MA, Auriola S, Nyman TA, Alafuzoff I, Pirttilä T (2005) Proteomic analysis of glial fibrillary acidic protein in Alzheimer's disease and aging brain. Neurobiol Dis 20: 858-870.

[61] Pamplona R, Dalfó E, Ayala V et al., Proteins in human brain cortex are modified by oxidation, glycoxidation, and lipoxidation. Effects of Alzheimer disease and identification of lipoxidation targets, J Biol Chem, 2005, 280, 21522-21530

[62] Muntané G, Dalfó E, Martínez A et al., Glial fibrillary acidic protein is a major target of glycoxidative and lipoxidative damage in Pick's disease, J Neurochem, 2006, 99, 177-185

[63] Martínez A, Carmona M, Portero-Otin M et al., Type-dependent oxidative damage in frontotemporal lobar degeneration: cortical astrocytes are targets of oxidative damage, J Neuropathol Exp Neurol, 2008, 67, 1122-1136

[64] Santpere G, Ferrer I, Delineation of early changes in cases with progressive supranuclear palsy-like pathology. Astrocytes in striatum are primary targets of tau phosphorylation and GFAP oxidation, Brain Pathol, 2009, 19, 177-187